Development 133, 4517-4526 (2006) doi:10.1242/dev.02642

Intrinsic chiral properties of the *Xenopus* egg cortex: an early indicator of left-right asymmetry?

Michael V. Danilchik*, Elizabeth E. Brown and Kristen Riegert

Vertebrate embryos define an anatomic plane of bilateral symmetry by establishing rudimentary anteroposterior and dorsoventral (DV) axes. A left-right (LR) axis also emerges, presaging eventual morphological asymmetries of the heart and other viscera. In the radially symmetric egg of *Xenopus laevis*, the earliest steps in DV axis determination are driven by microtubule-dependent localization of maternal components toward the prospective dorsal side. LR axis determination is linked in time to this DV-determining process, but the earliest steps are unclear. Significantly, no cytoskeletal polarization has been identified in early embryos capable of lateral displacement of maternal components. Cleaving *Xenopus* embryos and parthenogenetically activated eggs treated with 2,3-butanedione monoxime (BDM) undergo a dramatic large-scale torsion, with the cortex of the animal hemisphere shearing in an exclusively counterclockwise direction past the vegetal cortex. Long actin fibers develop in a shear zone paralleling the equator. Drug experiments indicate that the actin is not organized by microtubules, and depends on the reorganization of preexisting f-actin fibers rather than new actin polymerization. The invariant chirality of this drug response suggests a maternally inherited, microfilament-dependent organization within the egg cortex that could play an early role in LR axis determination during the first cell cycle. Consistent with this hypothesis, brief disruption of cortical actin during the first cell cycle randomizes the LR orientation of tadpole heart and gut.

KEY WORDS: Axis formation, Left-right asymmetry, *Xenopus laevis*, Actin, Microtubule, Egg, Cytoskeleton

INTRODUCTION

The first steps in embryonic patterning involve the specification of major body axes. In many organisms, these early events are accomplished by the localization or sequestration of maternally synthesized proteins and mRNAs. Such localizations are mediated by specific cytoskeletal structures or organizations during late oogenesis or early development. For example, during oogenesis in *Xenopus laevis*, microtubules, microfilaments and cytokeratins play specific roles in transporting or anchoring maternal mRNAs to various sites along the animal-vegetal axis of the oocyte (Kloc and Etkin, 1995; Klymkowsky et al., 1991; Pondel and King, 1988; Yisraeli et al., 1990). Later, during the first embryonic cell cycle, the dorsoventral (DV) axis is superimposed on this oogenetic animal-vegetal polarity via a microtubule-dependent rotation of the cortex relative to the inner cytoplasm (Weaver and Kimelman, 2004). The rotation displaces vegetal pole determinants toward the equator on the side opposite the sperm entry point (Weaver and Kimelman, 2004); the result is the initiation of a dorsoanterior-specific program of gene expression (Rowning et al., 1997) via the localized suppression of β-catenin degradation (Miller et al., 1999). With the appearance of the DV axis, anteroposterior and mediolateral dimensions emerge as well; thus, the direction of vegetal-cortical rotation defines the embryonic plane of bilateral symmetry. Externally, the embryo remains bilaterally symmetric, but internally, the various visceral organ systems develop with consistent left-right (LR) asymmetries. The origins of these LR asymmetries remain elusive.

Studies in several vertebrate systems indicate that latter steps in the development of LR asymmetric patterns follow well-conserved genetic pathways (Kramer and Yost, 2002; Levin, 2004). Left-sided *nodal* expression in the early neurula stage is the earliest conserved transcriptional event thus far recognized, and in many organisms *nodal* induction requires left-directed ciliary flow in the node, the floorplate or Kupffer's vesicle (Essner et al., 2005). The case of *Xenopus* may be somewhat unusual, in that asymmetries across the incipient embryonic midline develop prior to the onset of zygotic gene expression, and clearly precede the appearance of any cilia. For example, an asymmetry in Vg1-signaling, important for normal LR patterning, is established by the 16-cell stage (Hyatt and Yost, 1998). The possibility that the vegetal-cortical microtubule array is biased to generate such LR differences across the incipient midline during the first cell-cycle rotation was raised some time ago (Yost, 1991), but no consistent structural asymmetry has ever been reported. Assuming that the orientation of the microtubule array is directly related to that of the DV axis, it is difficult to understand how left and right halves could utilize this presumably symmetrical geometry to achieve material differences during the pre-cleavage period. However, maternal products involved with LR symmetrization, such as 14-3-3E (Bunney et al., 2003) and H^+-V-ATPase (Adams et al., 2006), become localized asymmetrically during early cleavage, indicating that a mechanism to localize maternal determinants must operate far upstream in the LR-specification pathway.

In this report, we address the possibility that the maternal cytoskeleton provides an unambiguous directional cue that serves to redistribute maternal components of the LR pathway unidirectionally along the mediolateral dimension during or shortly after the establishment of bilateral symmetry. Because the mediolateral dimension is not fixed until after fertilization, this directional capacity must initially be distributed uniformly around the animal-vegetal axis. When we used BDM to interfere with cytokinesis in cleaving *Xenopus* embryos, we noticed that an unusual torsion occurred between separating blastomeres, with the animal pole of each cell rotating several tens of degrees counterclockwise relative to the other, yielding a consistently chiral cleavage pattern. Investigating this effect further, we found that

Department of Integrative Biosciences, Oregon Health and Science University, Portland, OR 97239-3097, USA.

*Author for correspondence (e-mail: danilchi@ohsu.edu)

Accepted 13 September 2006

BDM induces shear in a broad belt around the equatorial cortex of the embryo. In parthenogenetically activated eggs this shear resulted in a dramatic, consistently counterclockwise torsion between animal and vegetal hemispheres about the animal-vegetal axis. Contemporaneous with this torsion, a broad continuous array of actin fibers assembled in the equatorial cortex, with contractile fibers paralleling the equatorial plane. Microtubules were not required to modulate this reorganization of the cortex, as torsion and development of the microfilament array continued unabated following nocodazole treatment. Finally, disruption of the actin cortex with BDM during the first cell cycle yielded tadpoles with a high frequency of reversal in cardiac and visceral LR orientation. These results demonstrate the existence of an unambiguously chiral polarization of the maternally derived cortical actin. The geometry of this polarization indicates an oogenetically based mechanism to localize determinants asymmetrically across the incipient embryonic midline, and therefore constitutes one of the farthest-upstream elements yet described in the vertebrate LR-specification pathway.

MATERIALS AND METHODS

Egg and embryo culture

Adult *X. laevis* females were induced to ovulate and eggs were fertilized, dejellied and cultured in MMR/3 as previously described (Danilchik et al., 2003). In some experiments, embryos were devitellinated manually in dishes coated with 2% type V agarose. For parthenogenetic activation, spawned eggs or in vitro-matured oocytes were maintained at 18°C in full-strength MMR for up to 3 hours before stimulation via a 3-second pulse of 3 volts, 800 mA DC. Activated eggs produced contractions of the animal cap about 7-10 minutes post-activation, and 'pre-cleavage' surface contraction waves at about 70-80 minutes post-activation, i.e. with the same timing as fertilized sibling eggs.

Timing of early embryonic events are normalized to the duration of the ~90 minute first cell cycle, with 0.0 NT (normalized time) denoting fertilization and 1.0 NT the onset of first cleavage.

GFP-actin labeling of oocytes

A GFP-actin sequence (Clontech) was inserted into the pCS107 vector, and transcribed and capped in vitro via mMessage mMachine (Ambion). Stage VI oocytes, harvested manually from adult *Xenopus* ovary, were injected with GFP-actin mRNA and cultured overnight in oocyte culture medium (50% Leibovitz L-15 containing glutamine, 15 mmol/l HEPES, pH 7.8, 1 μg/ml insulin, 50 units/ml nystatin, 100 μg/ml gentamycin and 100 units/ml penicillin/streptomycin). Oocytes expressing GFP-actin were subsequently matured by overnight exposure to 2 μg/ml progesterone, and then bathed in oocyte culture medium until activated electrically.

Drug treatments

Dejellied embryos were transferred into culture dishes containing 20 mmol/l BDM (Sigma) in MMR/3 at specified times following fertilization or parthenogenetic activation. For some experiments, embryos were transferred to dishes containing BDM and nocodazole (10 μg/ml), cytochalasin B (10 μg/ml), jasplakinolide (0.4 μg/ml) or latrunculin B (0.1 μg/ml) with up to 0.25% DMSO as vehicle. These concentrations had previously been determined to disrupt the contractile ring (not shown). Control experiments (not shown) indicated no effects of DMSO alone on cleavage, surface contractility, embryo viability or frequency of LR patterning defects.

Histochemical procedures

Fixation and staining protocols for microfilaments and microtubules were modified from previously published methods (Danilchik et al., 2003; Roeder and Gard, 1994). Embryos and activated eggs were fixed at various stages in BRB (1 mmol/l $MgCl_2$, 5 mmol/l EGTA, 80 mmol/l K-PIPES, pH 6.8) containing 3.7% paraformaldehyde, 0.25% glutaraldehyde and 0.2% Triton X-100 for 2 hours to overnight at 4°C. Specimens were then rinsed for several hours in three to four changes of NTBS (155 mmol/l NaCl, 10 mmol/l Tris-Cl, 0.1% NP-40, pH 7.4), and then devitellinated as needed. Specimens were stained overnight at 4°C with rhodamine phalloidin or Alexa 546 phalloidin (Molecular Probes, Inc.), rinsed for several hours with several changes of NTBS, and placed in shallow depression slides, in NTBS, under coverslips for viewing via confocal microscopy. For microtubule staining, specimens were incubated with anti-αβ-tubulin (Biogenesis) followed by Alexa-conjugated secondary antibodies as previously described (Danilchik et al., 2003).

Microscopy and time-lapse recording

To observe furrow morphology, still images were taken of cleaving embryos fixed briefly in Bouin's fixative and rinsed in alkaline 50% ethanol. Stills and time-lapse sequences (12 seconds/frame) of live embryos and activated eggs were recorded with an Optronics Microfire (TM) camera mounted on an Olympus SZH stereoscope. Side views were obtained by recording through a small mirrored 45° prism (Melles Griot) placed beside upright embryos or activated eggs. Time-lapse sequences were converted to Quicktime (Apple) with JPEG compression. Upright confocal imaging of live and fixed specimens was via a BioRad Radiance 2100 on a Nikon E800 microscope. Confocal time-lapse sequences were captured at 6 seconds/frame. For analysis, sequences were converted to TIFF stacks using ImageJ (http://rsb.info.nih.gov/ij/).

Assay for cardiac left-right orientation

Tadpoles were raised to stage 45-47 (Nieuwkoop and Faber, 1994), anesthetized with MS-222 (0.01%) and scored visually for direction of heart looping. As noted by others (Bunney et al., 2003), reversal of looping of gut and other visceral organs frequently accompanies that of heart. For this study, however, scoring was confined to cardiac looping itself.

RESULTS

Butanedione monoxime induces a chiral blastomere-blastomere torsion

While screening various agents for inhibition of early cleavage, we discovered that BDM causes blastomeres of cleaving *Xenopus* zygotes to undergo an unusual, polarized torsion, leaving a striking chiral pattern in the pigmented animal hemisphere. Eggs were fertilized, dejellied and transferred at various times into culture medium containing 20 mmol/l BDM. When exposed to BDM near the end of the first cell cycle, cleavage commenced normally, with the cleavage furrow appearing first as a contractile band at the animal pole that steadily lengthened toward the equator. However, as cleavage progressed, two unusual motions occurred, resulting in the pigment patterns seen in Fig. 1A (see also Movie S1 in the supplementary material). Halfway through the first cleavage, the

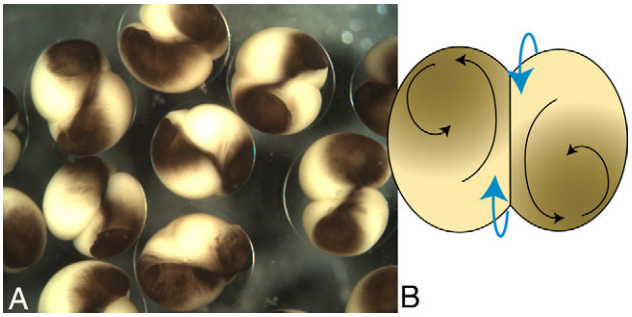

Fig. 1. BDM exposure late in the first cell cycle produces counterclockwise torsion of blastomeres during first cleavage. (**A**) *Xenopus* embryos were immersed in 20 mmol/l BDM at 75 minutes post-fertilization (0.83 NT). In every embryo, each blastomere rotates relative to the other in a counterclockwise direction, resulting in a characteristic chiral pattern. (**B**) The counterclockwise twisting of the pigmented animal cortex of each blastomere relative to the animal-vegetal axis of the embryo (black arrows) produces an invariably counterclockwise torsion between blastomeres as they cleave (blue arrows).

surface of the animal hemisphere in each blastomere began twisting counterclockwise relative to the underlying vegetal hemisphere (black arrows, Fig. 1B). At the same time, the two blastomeres underwent mutual counterclockwise torsion, as though rotating past each other on the mitotic spindle axis (blue arrows, Fig. 1B). These two motions produced a reverse-∫ trail of pigment behind the twisting animal cortex of each blastomere. Interestingly, among hundreds of embryos examined, from dozens of similarly treated spawnings, we never encountered a corresponding mirror-image (clockwise) motion. This drug response therefore reflects an underlying chiral organization in the cytoskeleton of the zygote.

Normal first cleavage also has a chiral morphology

While investigating the effects of BDM on cleavage, we observed that normal, untreated *Xenopus* zygotes also displayed – albeit transiently – a strongly chiral bias in at least one aspect of cleavage furrow morphology. During cleavage, prominent puckers or stress folds develop along the margins of the advancing cleavage furrow. Initially, these stress folds are spaced evenly, and more or less symmetrically, across the furrow. As new membrane expansion begins in the cleavage plane, the stress folds converge onto two apices at the midpoint of the furrow margins near the animal pole. These apices commonly become offset from the animal pole by several tens of microns (Fig. 2A-E, arrows). Although the offset is easier to see in fixed eggs (Fig. 2A-C), it is not a fixation artifact, as revealed via time-lapse microscopy (not shown), and is briefly visible even in eggs that have not been devitellinated or dejellied (Fig. 2D,E, respectively). Remarkably, the direction of offset is not random, as one might have expected from this confirmed deuterostome embryo. To quantify this chiral behavior, we fixed large numbers of embryos from three separate spawnings at the first sign of cleavage. Bouin's fixative was found to be ideal for this procedure, as it fixes tissues rapidly and preserves overall morphology with minimal shrinkage. Most blastomeres (about 63%; n=165) rotated counterclockwise to each other. Exceedingly few individuals (1%) displayed a clockwise torsion. The remaining 36% included both those that appeared to be symmetrical (no torsion) and those that had been fixed slightly too late or too early to be scorable. Thus, normal first cleavage in *Xenopus* is inherently chiral. The dramatic torsion elicited by BDM described above appears to exaggerate or enhance this inherent chiral property of the egg cortex.

BDM induces ectopic cortical microfilament bundling

To investigate the cytoskeletal basis for the chiral torsion produced by BDM treatment, we first examined the cortical microfilament distribution in cleaving embryos at various times following drug exposure (Fig. 3). Treatment early in the first cell cycle (<0.4 NT) sometimes produced chaotic and highly dynamic cortical blebbing, particularly in the animal hemisphere (Fig. 3A). In many cases, the blebbing became so vigorous that the surface ripped open. Fluorescent phalloidin staining revealed a complete reorganization of the normally amorphous cortical f-actin into long microfilaments

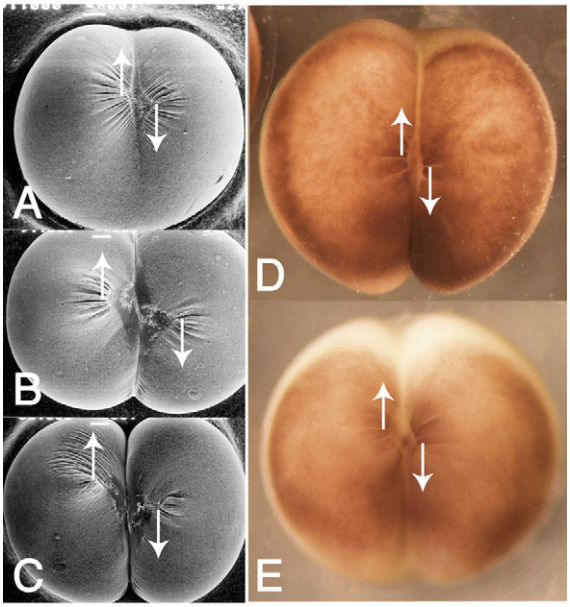

Fig. 2. Normal first cleavage in *Xenopus* is chiral and not mirror-image symmetric. Both fixed (**A-C**) and live (**D-E**) embryos, untreated, reveal a slight counterclockwise torsion of the two blastomeres during cleavage furrow advance. The apex of each furrow margin, i.e. the site at which furrowing began, becomes offset relative to the corresponding point in the opposite blastomere (arrow bases). By mid-cleavage (C), the offset between devitellinated blastomeres may be as much as 150 μm. Although the asymmetry is accentuated by dejellying (D) or removal of the vitelline envelope, even embryos with undisturbed jelly coats (E) display the same chirality. The offset normally becomes obscured as cleavage proceeds and the stress folds relax.

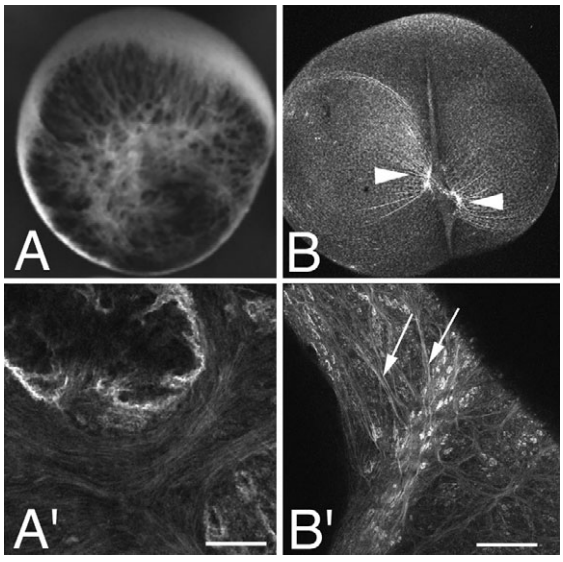

Fig. 3. Microfilaments bundle ectopically in cortex following BDM treatment. *Xenopus* zygotes were exposed to 20 mmol/l BDM beginning at 0.38 NT (**A**) or 0.94 NT (**B**) after fertilization. The earlier BDM exposure caused extensive contraction and irregular blebbing in the animal cap (A). Rhodamine-phalloidin staining of the surface, showing long, branching ectopic microfilament bundles (**A′**). The later BDM exposure induced torsion between the two cleaving blastomeres (offset indicated by paired arrowheads in B) and extensive bundling of ectopic actin fibers that branched and spread across cortex from the growing edge of the contractile ring (arrows in **B′**). Scale bars: 10 μm in A′; 75 μm in B.

arranged in broad, sometimes branching, swaths of parallel actin fibers around individual blebs (Fig. 3A′). Exposure to BDM at the onset of cleavage produced an enhanced offset of the apical stress folds (arrowheads in Fig. 3B), indicating the counterclockwise torsion between blastomeres described above. Thick, ramified microfilament bundles fanned out ectopically as extensions of the leading tips of the contractile ring (Fig. 3B′, arrows). Despite this large-scale ectopic remodeling of the cortical actomyosin, the contractile ring itself developed and advanced more or less normally, and was evidently capable of sufficient contractility to initiate furrowing in treated embryos. In summary, BDM treatment appears to provoke or enhance an alignment of ectopic, contractile cortical actin fibers, but not to interfere directly with contractile ring assembly or its function.

Parthenogenetically activated eggs undergo BDM-induced torsion of cortex

The fact that both treated and untreated embryos exhibited a slight chirality during cleavage raised the possibility of influence by the mitotic apparatus, as occurs in spiralian embryos (Shibazaki et al., 2004). To learn whether BDM-induced chirality exists in the absence of a mitotic spindle, we parthenogenetically activated dejellied *Xenopus* eggs in the presence of BDM. Eggs activated by electrical or osmotic shock initiate cdc2/cyclin-dependent cytoplasmic and DNA-replication cycles (Perez-Mongiovi et al., 1998; Rankin and Kirschner, 1997), raise a fertilization envelope and undergo nearly normal, albeit delayed, cortical surface contraction waves, but ultimately fail to cleave because they lack a mitotic spindle. BDM induces activated eggs to undergo a rapid, invariably counterclockwise torsion, and produce a striking spiral pattern of pigmentation in the animal hemisphere (Fig. 4; see also Movie S2 in the supplementary material). Thus, the chiral torsion of the egg cortex does not require presence of the sperm centrosome or mitotic spindle.

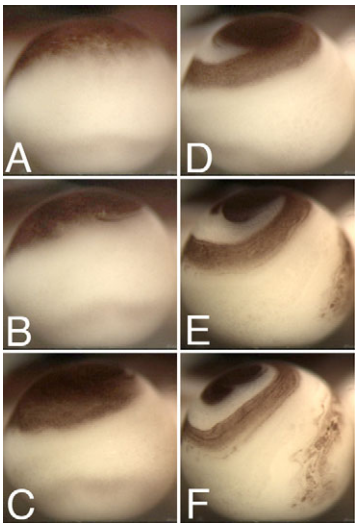

Fig. 4. Cortical torsion occurs in parthenogenetically activated eggs. (**A-F**) Eggs were parthenogenetically activated and, from 75 minutes post-activation (~0.79 NT) onward, bathed continuously in 20 mmol/l BDM. Activated egg, viewed from the side through two cleavage cycle equivalents (frames approximately 10 minutes apart), developed a spiraled pigment pattern in the animal hemisphere as the surface rotated left to right (counterclockwise).

BDM-induced torsion does not require microtubules

Although parthenogenetically activated eggs lack a sperm centrosome, they still generate a microtubule monaster and a vegetal-cortical microtubule array, and thus microtubule ends could still be interacting with, and potentially influencing, the cortex during BDM treatment. Because microtubules are known to modulate the flow of cortical actomyosin of *Xenopus* oocytes treated with phorbol ester (Benink et al., 2000; Canman and Bement, 1997), we tested whether the BDM-induced torsion could develop in the continuous presence of nocodazole, a microtubule-depolymerizing agent. As shown in Fig. 5, microtubules are not required for this torsional activity: a steady counterclockwise rotation of the animal caps continued in BDM/nocodazole-treated eggs for at least 4 hours, through several cell-cycle equivalents. Thus, the chiral response of the cortex to BDM does not require recent contact with microtubules. To test whether microtubules present before activation might have been important for cueing the post-activation BDM response, we pretreated eggs for several hours with nocodazole. After activation in the presence of BDM, pretreated eggs underwent essentially the same chiral torsion as described above (not shown). In summary, the chiral responsiveness of the cortex of the egg does not depend on the presence of microtubules at any time before activation or during the first cell cycle, and therefore seems to be an intrinsic property of cortical actin itself.

Parallel bundles of cortical actin assemble in the equatorial shear zone

To understand the cytoskeletal basis of the animal hemisphere rotation, we used a mirrored 45° prism to obtain side views of the equatorial region of living eggs treated with BDM. Analysis of video time-lapse recordings indicated that the surfaces of both animal and vegetal hemispheres undergo cortical rearrangements, but a zone of particularly extensive shear develops between the two hemispheres in a 300 μm-wide belt below the equatorial pigment boundary. To illustrate the extent and rate of this shear, individual pigment granules initially spaced approximately 100 μm apart along an arbitrary animal-vegetal meridian served as surface marks that were tracked for 20 minutes in a representative side-view time-lapse movie (see Movie S3 in the supplementary material). As shown in Fig. 6, the upper part of the animal hemisphere underwent a relatively small amount of localized deformation as it rotated atop

Fig. 5. Cortical torsion does not require interaction with microtubules. The eggs were incubated continuously for 4 hours (about four cell-cycle equivalents) in the presence of 20 mmol/l BDM and 10 μmol/l nocodazole. The cortical pigment pattern indicates counterclockwise rotation through several revolutions.

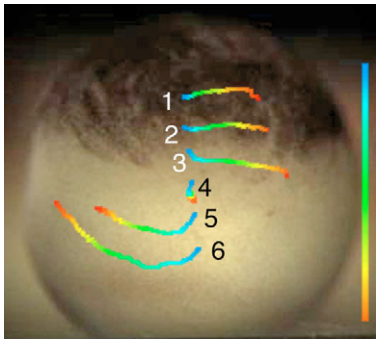

Fig. 6. A broad shear zone develops at the equator of BDM-treated activated eggs. The frame from a side-view time-lapse sequence spanning a 20 minute period at the beginning of torsion (see Movie S3 in the supplementary material). Motion of individual pigment granules (marks 1-6) traced via time-lapse is indicated by colored tracks. The colored bar indicates a 20 minute time interval (blue: start of tracking; red: +20 minutes).

the vegetal hemisphere. The three adjacent marks above the equator (marks 1-3) traveled at about the same speed and therefore remained in relatively close proximity, indicating that the circumpolar animal hemisphere surface rotated more or less as a coherent unit. By contrast, marks below the pigmentation boundary (marks 4-6) underwent a much larger amount of relative motion, indicating that a broad shear zone develops in the equatorial zone. Considerable relative translocation of surface marks occurred across this zone. For example, marks 3 and 5, initially apart vertically only 210 μm across the shear zone, became separated laterally by more than 615 μm in the 20-minute period – a horizontal displacement rate of at least 30 μm/minute. Nearer the vegetal pole, horizontal movement was somewhat slower: marks 4 and 5 separated laterally from each other at about 16 μm/minute; marks 5 and 6 separated at about 6 μm/minute. Thus, relative rates of horizontal displacement varied several fold along the animal-vegetal meridian, with the fastest rates of shear at the equator.

As demonstrated above, the BDM-induced lateral shear can occur in the absence of microtubules, suggesting that cortical microfilaments respond more or less independently of other cytoskeletal influences. We examined the distribution of cortical f-actin in both fixed and live eggs treated with BDM and nocodazole. Fig. 7A shows a parthenogenetically activated egg fixed while undergoing drug-induced torsion. The egg was then stained with rhodamine phalloidin and examined via confocal microscopy (Fig. 7B). F-actin in the animal cap was organized into irregular clumps and along the edges of blebs, similar to that previously described (see Fig. 3A, above). By contrast, in regions of maximal shear near the equator, we found broad parallel arrays of microfilaments (Fig. 7C). These bundles were typically coincident with long circumferential grooves paralleling the shear (Fig. 7B). The presence of the grooves indicates that the microfilament bundles exert considerable circumferential constriction. Thus, the actin array is probably tethered to the plasma membrane and operates via filament sliding, as in the contractile ring.

To observe the behavior of this microfilament array in vivo, we injected stage VI oocytes with capped mRNA encoding GFP fused to actin. After incubating overnight, GFP-actin expressing oocytes were matured with progesterone and then electrically activated as above in the presence of BDM and nocodazole. These labeled oocytes underwent essentially the same large-scale counterclockwise torsion as activated eggs, with shearing across a broad equatorial zone as described above. Large numbers of discrete, actin-containing microfilament bundles aligned into broad arrays paralleling the shear (Fig. 8A). Individual fibers within the array had an apparent thickness of about 0.5 μm and they ranged in length from about 4 μm to at least 45 μm (Fig. 8B). Much longer fibers were within the array, but because the surface of the live egg continually undulated, individual fibers could not be traced for long distances in any single confocal section. Analysis of representative transects across the array indicates relatively uniform spacing (0.90±0.08 μm) of individual filament bundles (Fig. 8C), similar to previous measurements of microfilaments in the contractile bands of *Xenopus* cleavage furrows (Noguchi and Mabuchi, 2001). We analyzed motions of individual fibers in confocal time-lapse movies and measured a nearly uniform sliding of individual fibers past each other at an average rate of 0.03 μm/minute (see Fig. S1 and Movie S4 in the supplementary material). Importantly, no fibers slid in the opposite direction. Thus, the rapid counterclockwise rotation of the animal cap surface seen macroscopically results from the cumulative action of incremental and unidirectional sliding of adjacent microfilament bundles in the equatorial belt.

BDM-induced torsion requires f-actin, but not ongoing actin assembly

The contractile band of *Xenopus* zygotes develops both by recruitment of cortical actin and new polymerization in situ at the growing furrow tips (Noguchi and Mabuchi, 2001). As a preliminary test of whether the equatorial microfilament array in BDM-treated embryos develops via new assembly or recruitment from preexisting cortical f-actin, we exposed activated eggs undergoing torsion to various microfilament inhibitors. At doses previously determined to be effective at halting cytokinesis, latrunculin B (1 μg/ml) essentially abolished all cortical movements, confirming that the torsion is indeed dependent on the presence of microfilaments. However, cytochalasin B (10 μg/ml) and jasplakinolide (0.4 μg/ml), agents that respectively block and stabilize actin assembly, had no effect on torsion, indicating that the equatorial actin array develops largely via reorganization of preexisting cortical microfilaments.

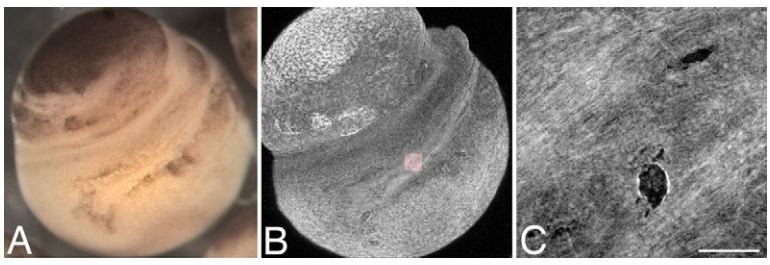

Fig. 7. Long microfilament bundles parallel the equatorial shear. A parthenogenetically activated egg treated with BDM/nocodazole observed to be undergoing torsion (**A**) was fixed and stained with rhodamine-phalloidin and examined via confocal microscopy (**B**). Bundles of cortical microfilaments parallel the direction of shear in the equatorial region. The region indicated by the colorized box is shown at higher magnification (**C**). A small post-fixation tear in the surface (dark spot) reveals relatively little organized f-actin beneath the cortex. Scale bar in C: 30 μm.

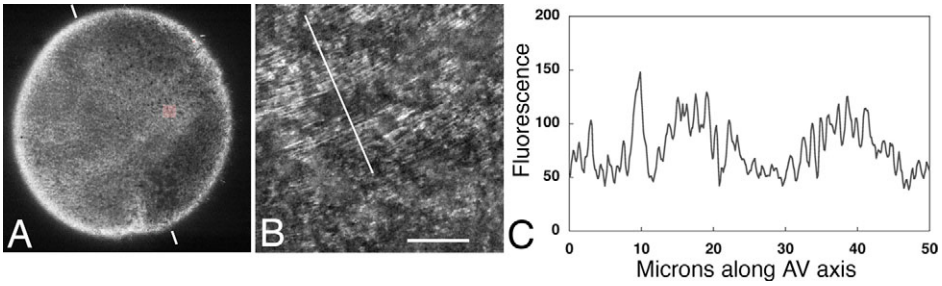

Fig. 8. Cortical microfilament bundles slide past each other, paralleling the direction of shear. (**A**) Equatorial view via confocal microscopy of an egg matured from an oocyte injected with GFP-actin mRNA. The egg was parthenogenetically activated and incubated in BDM/nocodazole. White bars indicate the orientation of the animal-vegetal axis. (**B**) The colorized region is examined at higher magnification, showing GFP-decorated microfilaments oriented in a band paralleling the equator. (**C**) The fluorescence intensity profile along a white transect in B paralleling the animal-vegetal meridian. The distribution of intensity maxima indicates relatively uniform spacing of GFP-actin microfilament bundles. Scale bar in B: 15 μm.

Actin cortex and left-right axis specification

The consistent directionality of the BDM-induced equatorial microfilament belt indicates the presence of an endogenous circumferential polarization within the cortex of the egg. Whatever the physical nature of the initial polarization, its orientation suggests a potential actin-dependent mechanism for breaking the mirror-image symmetry of the zygote during the first cell cycle. We hypothesized that this chiral polarization reflects a transport mechanism used by the zygote or early-cleavage embryo to localize components of a LR axis-specifying pathway. If this hypothesis is correct, then disrupting the actin cytoskeleton early in development should result in LR patterning defects. Supporting this idea, it has already been demonstrated that exposing *Xenopus* embryos to sublethal doses of latrunculin B for several hours during cleavage stages results in randomized cardiac and gut LR patterning (Qiu et al., 2005).

BDM treatment causes rapid and dramatic reorganization of cortical actin, and, unlike latrunculin, the compound can be washed out quickly, allowing treated embryos to recover and develop to tadpole stage. Thus, to learn more precisely when actin might play a role in LR patterning, we pulse-treated *Xenopus* embryos with BDM at various stages during early development, and scored them at stage 45-47 (Fig. 9A) for orientation of the heart. As shown in Table 1, LR patterning was sensitive to 20 minutes of BDM exposure during the middle portion of the first cell cycle (between 0.25 and 0.67 NT), resulting in a high frequency of LR reversal of heart (Table 1) and gut (not shown), often without any sign of DV patterning defects (Fig. 9B). Little effect on heart orientation resulted when embryos were treated before 0.25 NT. Similarly, embryos exposed after first cleavage produced no cardiac or axis patterning defects at all. To summarize, LR pattern specification of the heart can be disturbed by abrupt disruption of the cortical actin during a discrete period of the first cell cycle. This period corresponds roughly to the time of the microtubule-dependent vegetal rotation.

In the experiment above, survival to a scorable tadpole stage varied considerably with time of exposure within the first cell cycle for different, stage-specific, reasons. Late first cell cycle treatments compromised cleavage itself, producing embryo loss before gastrulation. By contrast, early first cell cycle treatments often produced embryos with significant amounts of ectopic dorsoanterior development, sometimes including conjoined twins and radialized hyperdorsal forms (Fig. 10A). Because this range of defects closely resembled the hyperdorsoanterior series resulting from D_2O treatment during the first cell cycle (Kao and Elinson, 1988; Scharf et al., 1989), we suspected that the cortical rearrangements induced by early BDM treatment might directly perturb the vegetal-cortical microtubule array. Comparison of the cortical microtubules in untreated and BDM-treated zygotes (Fig. 10B,C, respectively) confirmed this idea: in early-treated embryos, the microtubule array sometimes became radialized, with microtubule bundles sweeping up past the equator along multiple meridians. This finding suggests interaction between the cortical actin and the highly labile microtubule array during its initial growth in the first cell cycle.

The brief, early BDM treatments that randomized cardiac and gut orientation were not of sufficient duration to produce equatorial torsion described above, but clearly were sufficient to redirect normal LR patterning. To observe the actual extent of cortical actin reorganization induced by brief, heart-randomizing treatments, embryos were fixed during the course of 20 minutes exposure to

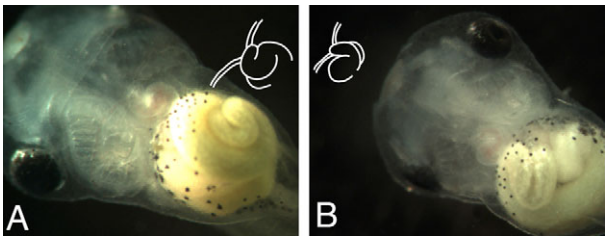

Fig. 9. BDM treatment can randomize cardiac and gut left-right patterning. (**A**) An untreated stage-47 tadpole displays normal situs of heart and gut coiling. (**B**) A tadpole exposed to 20 mmol/l BDM for 20 minutes during the first cell cycle displays reversed cardiac and gut organizations, with otherwise normal body patterning. Insets show outlines of normal (A) and reversed (B) cardiac outflow tract and ventricle.

Table 1. Effect of BDM on cardiac left-right patterning

Onset of treatment	Sample (*n*)	% Heart reversal	*P*
None	325	2	~
⩽0.25 NT	76	4	0.621
0.25-0.45 NT	93	18	<0.001
0.45-0.67 NT	124	23	<0.001
0.67-1.0 NT	181	3	0.899
Post-cleavage	232	0	0.186

Embryos were dejellied after fertilization and exposed for 16-20 minutes to 20 mM BDM at the various times indicated. Heart orientation was scored as normal or reversed among tadpoles surviving to stage 45-47.
P values are based on standard χ^2 analysis.

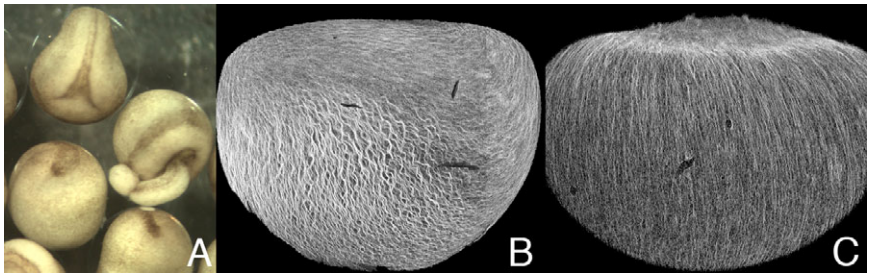

Fig. 10. Hyperdorsalization results from radialized vegetal microtubule array. (**A**) Embryos treated with 20 mmol/l BDM for 20 minutes during the first cell cycle displayed a range of conjoined-twin and radialized hyperdorsal morphologies. (**B**) A normal vegetal-cortical microtubule array, seen from the side in a whole-mount embryo immunostained for αβ-tubulin via confocal microscopy. The specimen is oriented with the animal pole up, sperm entry point to the right, and thus prospective dorsal to the left. (**C**) A vegetal-cortical microtubule array in a BDM-treated sibling displaying the extreme hyperdorsal phenotypes seen in A. The specimen orientation is the same as that for B.

BDM (Fig. 11A1-A3), and then stained with rhodamine-phalloidin for whole-mount confocal microscopy. Cortical contraction first became noticeable about 10 minutes after exposure to BDM, with the appearance of a distinctive horizontal constriction or sulcus at the equatorial pigment boundary (Fig. 11A2,A3, arrows). Interestingly, in all cases observed (n>30 from three separate spawnings), the sulcus first appeared on the side opposite to the sperm entry point (SEP), i.e. prospective dorsal marginal zone. Confocal microscopy revealed that this dorsal sulcus is enriched with microfilaments (Fig. 11B), arranged linearly and running parallel to the equator (Fig. 11C). Thus, in contrast to parthenogenetically activated eggs that produce a uniformly circumferential microfilament array at the equator, the zygotes develop a microfilament array only on the prospective dorsal side.

As shown above, BDM exposure induces ectopic microfilament bundling into long cortical arrays, largely from preexisting f-actin. We suspected that the dorsal equatorial zone might constitute a local source of actin for BDM-induced reorganization during the middle of the first cell cycle. This possibility was confirmed by observing the distribution of rhodamine-phalloidin staining in untreated zygotes fixed at various times following fertilization. Fig. 11D,E shows animal and vegetal surfaces, respectively, of a single untreated zygote fixed at 75 minutes post-fertilization (a sibling of the BDM-treated zygote shown in Fig. 11B). Whether viewed from above or below, the surface on the anti-SEP side (corresponding to the prospective dorsal marginal zone) stained significantly brighter than that of the SEP side (the prospective ventral marginal zone). Based on examination of several dozen embryos of various stages, this

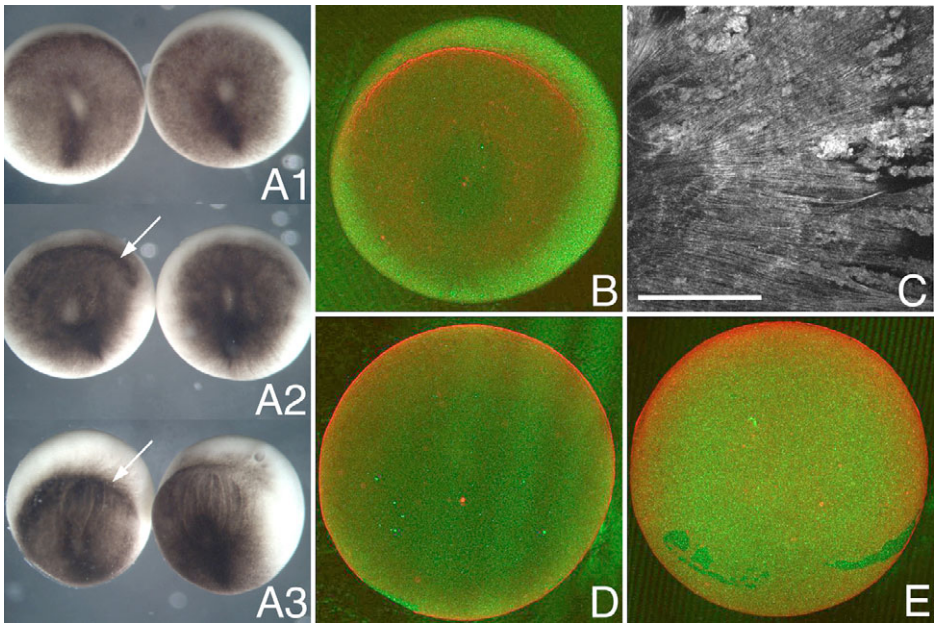

Fig. 11. Cortical f-actin in the dorsal marginal zone reorganizes to form a contractile equatorial band following BDM treatment. (**A**) Embryos were exposed to 20 mmol/l BDM beginning at 55 minutes post-fertilization and fixed 5, 10 and 20 minutes later (60, 65, 70 minutes post-fertilization; **A1-A3**, respectively). Each develops a horizontal sulcus, indicating surface contraction, on the side opposite the SEP (prospective dorsal marginal zone) (arrows in A2, A3). (**B**) Phalloidin-stained zygote, fixed at 75 minutes (20 minutes after BDM exposure) viewed in whole-mount via confocal microscopy; same orientation as zygotes in A. Rhodamine-phalloidin (red) stains equatorial sulcus brightly. Green reflection mode provides background, primarily to indicate that cortical pigment is not obscuring the view of cortical actin. (**C**) Detail of the surface at the edge of the sulcus, showing equatorially aligned microfilaments. Scale bar: 60 μm. (**D**,**E**) Animal and vegetal surfaces, respectively, of untreated zygote, fixed 75 minutes post-fertilization and stained with rhodamine-phalloidin, showing enrichment of cortical f-actin on the dorsal marginal zone.

dorsal accumulation represents an approximately twofold enrichment of actin relative to the ventral side. It develops concomitantly with the first cell cycle rotation from a distribution that is uniform before 40 minutes post-fertilization, and is microtubule-dependent (not shown). To summarize, surface actin capable of reorganization into a polarized, equatorial microfilament array accumulates onto the prospective dorsal marginal during a period in which the DV axis becomes established. Perturbing this actin distribution disrupts normal LR patterning of heart and viscera.

DISCUSSION

The *Xenopus* egg is cylindrically symmetric until fertilization, when the site of sperm entry superimposes the DV and LR body dimensions onto the original animal-vegetal axis (Manes and Elinson, 1980). Any maternal component involved with an upstream step in LR patterning would have to have an initially uniform distribution around the animal-vegetal axis, ready to undergo a useful (i.e. consistently orthogonal to the midsagittal plane) localization only during or shortly after DV specification. It has been hypothesized (Yost, 1991) that the vegetal-cortical microtubule array could accomplish this orthogonal bias, if the orientation of the microtubule deviated from the midsagittal plane. However, years of study by numerous investigators have revealed no consistent structural asymmetries in the vegetal-cortical array (Houliston and Elinson, 1991; Larabell et al., 1996; Marrari et al., 2003; Vincent et al., 1987) or of the locomotion of particles along it (Miller et al., 1999). Nevertheless, early asymmetries important in LR patterning do develop during prezygotic development. For example, vegetally localized maternal proteins and mRNAs enrich asymmetrically across the embryonic midline during early cleavage stage (Adams et al., 2006; Bunney et al., 2003). By the four-cell stage, blastomeres are already asymmetric with respect to serotonin signaling (Fukumoto et al., 2005). Interestingly, these localizations are sensitive to sublethal, chronic doses of the microfilament-depolymerizing drug latrunculin B.

There are a number of ways in which BDM might affect actin-dependent motion in the cortex of the early embryo. BDM reportedly functions as a low-affinity myosin ATPase inhibitor (Cramer and Mitchison, 1995), but in some situations may also act by interfering with unspecified non-ATPase functions of nonmuscle myosin II (Forer and Fabian, 2005). These potential myosin-disrupting effects are difficult to reconcile with the observed unidirectional sliding of microfilaments past each other through the cortex. Moreover, eggs exposed to a number of higher-affinity myosin inhibitors, including blebbistatin and ML7, did not exhibit any effects similar to that of BDM (M.V.D. and E.E.B., unpublished). Thus, it is worth considering the other known pharmacological effects of BDM on the cytoskeleton, including its inhibition of retrograde actin flow in lamellipodia (Lin et al., 1996; Zhou et al., 2002), reflecting direct interference with the assembly kinetics of actin (Valentijn et al., 2000). Alternatively, a recent study suggests that BDM blocks lamellipodial protrusion not by interfering with assembly kinetics per se, but rather by delocalizing actin-assembly components, principally the Arp2/3 complex, from the plasma membrane (Yarrow et al., 2003). A delocalization of actin assembly components would be consistent with the abundant ectopic microfilaments seen throughout the cortex of BDM-treated eggs, but as shown by our cytochalasin and jasplakinolide experiments, new assembly is not required to sustain the torsion once it has begun. Structural and functional similarity between the ectopic microfilament bands and the contractile ring suggest that BDM may be activating a rhoA-dependent pathway.

We do not yet understand the basis for the consistent directionality of the torsion elicited by BDM. One explanation would be that a cryptic chiral organization already exists on a large scale in the *Xenopus* egg cortical actin cytoskeleton by the time of fertilization, and that BDM simply reinforces it – e.g. by provoking polarized ectopic bundling onto preexisting, already oriented, microfilaments. Of course, this relegates the organizational problem back to oogenesis. Alternatively, the torsion may depend on chirality at a much smaller scale: the helicity of the microfilaments themselves. In this model, the ectopic bundling of cortical actin initiated by BDM would be chirally organized on a molecular level, incrementally conferring larger-scale chirality to the cortex as a whole.

There are no known cytoskeletal structures or organizations in *Xenopus* embryos that presage the surprising chiral response of the cortex to BDM. All previously described cortical motions of the early embryo organize around surface singularities, such as the animal pole or the sperm entry point, or symmetrical structures such as the mitotic spindle or vegetal cortical microtubule array. In general, they reflect preexisting maternal organization (the animal-vegetal axis of the oocyte) or later directional cues (the sperm centrosome and mitotic spindle). For example, the animal pole (site of meiotic cleavages) serves as a focus for large-scale, concentric surface contraction waves preceding first cell division. Subsequently, the fertilizing sperm centrosome provides a symmetry-breaking directional cue, culminating in the assembly of the cortical microtubule array perpendicular to the animal-vegetal axis that directs cytoplasmic motions important for DV axis specification. The unusual chiral behavior of the embryo cortex following BDM treatment reflects a topologically different arrangement: one that is organized circumferentially around the animal-vegetal axis. Whatever BDM may be doing at the biochemical level to elicit this response, it is important to recognize that the chiral behavior itself represents an endogenous vectorial cue in the cortical cytoskeleton, one that is potentially used by the pre-cleavage embryo for LR symmetrization. Thus, the initial left- or right-specific accumulation of critical maternal determinants might be accomplished by unidirectional tracking around the equator, and this large-scale handedness could function no matter where the sperm enters and the DV axis develops.

There are at least two ways in which circumferentially polarized cortical actin (or membrane-tethered microfilament nucleation sites) could function in symmetry breaking. One involves vesicle transport along microfilaments. Recent work in *Drosophila* implicates Myo1A, an unconventional myosin, in LR asymmetric gut looping (Hozumi et al., 2006). Although the suggested role for this myosin in *Drosophila* is in actin-dependent vesicle transport during a late stage of gut morphogenesis, a similar function could be served by circumferentially polarized cortical actin in *Xenopus* eggs. In this scenario, vesicles bearing components of a left- or right-determining pathway would shift unidirectionally around the equator. As we have shown, cortical actin becomes enriched at the dorsal marginal zone near the end of the first cell cycle. Thus, vesicles arriving at the marginal zone near the end of the first cell cycle (e.g. accompanying similar vesicles involved with dorsal specification) would have an opportunity to interact with microfilaments that, as we have shown, are capable of organizing horizontally into polarized arrays.

A second actin-dependent symmetry-breaking scenario in *Xenopus* embryogenesis is described in Fig. 12. In this model, actomyosin would produce a shear between deep and surface components about the animal-vegetal axis. This shear could be relatively minor, and yet accomplish a significant asymmetry

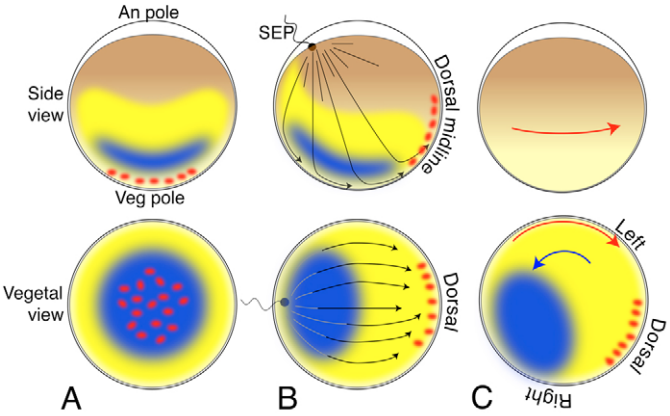

Fig. 12. Symmetry breaking accompanies DV axis specification during the first cell cycle. Top: side view. Bottom: vegetal view. (**A**) Before fertilization, deep (blue) and shallow (red) determinants are localized concentrically about the animal-vegetal axis. (**B**) After fertilization, the sperm centrosome initiates orientation of the vegetal-cortical microtubule array, producing a shift of dorsalizing components toward the incipient dorsal marginal zone, and a concomitant shift of deeper components and the yolk mass (yellow) toward the sperm entry point. The axial separation of the deep and shallow components defines the plane of bilateral symmetry. (**C**) An actin-dependent shift of surface counterclockwise relative to the deeper components produces significant material differences across the embryonic midline.

across the embryonic midline before cleavage. In the cartoon, maternal dorsal-specifying components (red dots), such as GSK-3 binding protein (Weaver et al., 2003) or xwnt 11 mRNA (Tao et al., 2005), are located in the vegetal cortex. Deeper in the cytoplasm, perhaps embedded in the yolk mass, are maternal elements (blue) involved with LR specification. These determinants could include, for example, H^+-V-ATPase proteins (Adams et al., 2006) or some component of Vg1 processing or signaling (Hyatt and Yost, 1998). Initially, the unfertilized egg has cylindrical symmetry about its animal-vegetal axis (Fig. 12A). Fertilization causes a microtubule-dependent shift of dorsal determinants toward the dorsal marginal zone (Schroeder et al., 1999; Yost et al., 1998), while the deeper determinants shift with the yolk mass toward the sperm entry point; the relative displacement of deep and shallow components defines the plane of bilateral symmetry (Fig. 12B). We suggest that a slight equatorial shift of the shallow components relative to those deeper in the cytoplasm would be sufficient to produce a significant de-symmetrization across the embryonic midline (Fig. 12C).

In summary, we have learned that exposure to millimolar concentrations of BDM causes massive reorganization of the actin cytoskeleton in the cortex of activated eggs and embryos of *Xenopus*, provoking a novel cortical movement resulting in a consistently counterclockwise torsion of the cortex. This chirality reveals a cryptic asymmetry in the cortical actin cytoskeleton of the egg that could provide cytoskeletal cueing to distinguish left from right in the early embryo.

This work was supported by the National Science Foundation (IBN-0110985 and IBN-0419664). Work done by K.R. was in partial fulfillment of her BA degree at Pacific University, with summer fellowship support from the M. J. Murdock Charitable Trust.

Supplementary material

Supplementary material for this article is available at http://dev.biologists.org/cgi/content/full/133/22/4517/DC1

References

Adams, D. S., Robinson, K. R., Fukumoto, T., Yuan, S., Albertson, R. C., Yelick, P., Kuo, L., McSweeney, M. and Levin, M. (2006). Early, H+-V-ATPase-dependent proton flux is necessary for consistent left-right patterning of non-mammalian vertebrates. *Development* **133**, 1657-1671.
Benink, H. A., Mandato, C. A. and Bement, W. M. (2000). Analysis of cortical flow models in vivo. *Mol. Biol. Cell* **11**, 2553-2563.
Bunney, T. D., De Boer, A. H. and Levin, M. (2003). Fusicoccin signaling reveals 14-3-3 protein function as a novel step in left-right patterning during amphibian embryogenesis. *Development* **130**, 4847-4858.
Canman, J. C. and Bement, W. M. (1997). Microtubules suppress actomyosin-based cortical flow in Xenopus oocytes. *J. Cell Sci.* **110**, 1907-1917.
Cramer, L. P. and Mitchison, T. J. (1995). Myosin is involved in postmitotic cell spreading. *J. Cell Biol.* **131**, 179-189.
Danilchik, M. V., Bedrick, S. D., Brown, E. E. and Ray, K. (2003). Furrow microtubules and localized exocytosis in cleaving Xenopus laevis embryos. *J. Cell Sci.* **116**, 273-283.
Essner, J. J., Amack, J. D., Nyholm, M. K., Harris, E. B. and Yost, H. J. (2005). Kupffer's vesicle is a ciliated organ of asymmetry in the zebrafish embryo that initiates left-right development of the brain, heart and gut. *Development* **132**, 1247-1260.
Forer, A. and Fabian, L. (2005). Does 2,3-butanedione monoxime inhibit nonmuscle myosin? *Protoplasma* **225**, 1-4.
Fukumoto, T., Kema, I. P. and Levin, M. (2005). Serotonin signaling is a very early step in patterning of the left-right axis in chick and frog embryos. *Curr. Biol.* **15**, 794-803.
Houliston, E. and Elinson, R. P. (1991). Patterns of microtubule polymerization relating to cortical rotation in Xenopus laevis eggs. *Development* **112**, 107-117.
Hozumi, S., Maeda, R., Taniguchi, K., Kanai, M., Shirakabe, S., Sasamura, T., Speder, P., Noselli, S., Aigaki, T., Murakami, R. et al. (2006). An unconventional myosin in Drosophila reverses the default handedness in visceral organs. *Nature* **440**, 798-802.
Hyatt, B. A. and Yost, H. J. (1998). The left-right coordinator: the role of Vg1 in organizing left-right axis formation. *Cell* **93**, 37-46.
Kao, K. R. and Elinson, R. P. (1988). The entire mesodermal mantle behaves as Spemann's organizer in dorsoanterior enhanced Xenopus laevis embryos. *Dev. Biol.* **127**, 64-77.
Kloc, M. and Etkin, L. D. (1995). Two distinct pathways for the localization of RNAs at the vegetal cortex in Xenopus oocytes. *Development* **121**, 287-297.
Klymkowsky, M. W., Maynell, L. A. and Nislow, C. (1991). Cytokeratin phosphorylation, cytokeratin filament severing and the solubilization of the maternal mRNA Vg1. *J. Cell Biol.* **114**, 787-797.
Kramer, K. L. and Yost, H. J. (2002). Cardiac left-right development: are the early steps conserved? *Cold Spring Harb. Symp. Quant. Biol.* **67**, 37-43.
Larabell, C. A., Rowning, B. A., Wells, J., Wu, M. and Gerhart, J. C. (1996). Confocal microscopy analysis of living Xenopus eggs and the mechanism of cortical rotation. *Development* **122**, 1281-1289.
Levin, M. (2004). The embryonic origins of left-right asymmetry. *Crit. Rev. Oral Biol. Med.* **15**, 197-206.
Lin, C. H., Espreafico, E. M., Mooseker, M. S. and Forscher, P. (1996). Myosin drives retrograde F-actin flow in neuronal growth cones. *Neuron* **16**, 769-782.
Manes, M. E. and Elinson, R. P. (1980). Ultraviolet light inhibits gray crescent formation in the frog egg. *Wilhelm Roux Arch. Dev. Biol.* **189**, 73-77.
Marrari, Y., Clarke, E. J., Rouviere, C. and Houliston, E. (2003). Analysis of microtubule movement on isolated Xenopus egg cortices provides evidence that the cortical rotation involves dynein as well as Kinesin Related Proteins and is regulated by local microtubule polymerisation. *Dev. Biol.* **257**, 55-70.
Miller, J. R., Rowning, B. A., Larabell, C. A., Yang-Snyder, J. A., Bates, R. L. and Moon, R. T. (1999). Establishment of the dorsal-ventral axis in Xenopus embryos coincides with the dorsal enrichment of dishevelled that is dependent on cortical rotation. *J. Cell Biol.* **146**, 427-437.
Nieuwkoop, P. D. and Faber, J. (1994). *Normal Table of Xenopus laevis (Daudin).* New York: Garland Publishing.
Noguchi, T. and Mabuchi, I. (2001). Reorganization of actin cytoskeleton at the growing end of the cleavage furrow of Xenopus egg during cytokinesis. *J. Cell Sci.* **114**, 401-412.
Perez-Mongiovi, D., Chang, P. and Houliston, E. (1998). A propagated wave of MPF activation accompanies surface contraction waves at first mitosis in Xenopus. *J. Cell Sci.* **111**, 385-393.
Pondel, M. D. and King, M. L. (1988). Localized maternal mRNA related to transforming growth factor beta mRNA is concentrated in a cytokeratin-enriched fraction from Xenopus oocytes. *Proc. Natl. Acad. Sci. USA* **85**, 7612-7616.
Qiu, D., Cheng, S. M., Wozniak, L., McSweeney, M., Perrone, E. and Levin, M. (2005). Localization and loss-of-function implicates ciliary proteins in early, cytoplasmic roles in left-right asymmetry. *Dev. Dyn.* **234**, 176-189.
Rankin, S. and Kirschner, M. W. (1997). The surface contraction waves of Xenopus eggs reflect the metachronous cell-cycle state of the cytoplasm. *Curr. Biol.* **7**, 451-454.

Roeder, A. D. and Gard, D. L. (1994). Confocal microscopy of F-actin distribution in Xenopus oocytes. *Zygote* **2**, 111-124.
Rowning, B. A., Wells, J., Wu, M., Gerhart, J. C., Moon, R. T. and Larabell, C. A. (1997). Microtubule-mediated transport of organelles and localization of beta-catenin to the future dorsal side of Xenopus eggs. *Proc. Natl. Acad. Sci. USA* **94**, 1224-1229.
Scharf, S. R., Rowning, B., Wu, M. and Gerhart, J. C. (1989). Hyperdorsoanterior embryos from Xenopus eggs treated with D2O. *Dev. Biol.* **134**, 175-188.
Schroeder, K. E., Condic, M. L., Eisenberg, L. M. and Yost, H. J. (1999). Spatially regulated translation in embryos: asymmetric expression of maternal Wnt-11 along the dorsal-ventral axis in Xenopus. *Dev. Biol.* **214**, 288-297.
Shibazaki, Y., Shimizu, M. and Kuroda, R. (2004). Body handedness is directed by genetically determined cytoskeletal dynamics in the early embryo. *Curr. Biol.* **14**, 1462-1467.
Tao, Q., Yokota, C., Puck, H., Kofron, M., Birsoy, B., Yan, D., Asashima, M., Wylie, C. C., Lin, X. and Heasman, J. (2005). Maternal wnt11 activates the canonical wnt signaling pathway required for axis formation in Xenopus embryos. *Cell* **120**, 857-871.
Valentijn, J. A., Valentijn, K., Pastore, L. M. and Jamieson, J. D. (2000). Actin coating of secretory granules during regulated exocytosis correlates with the release of rab3D. *Proc. Natl. Acad. Sci. USA* **97**, 1091-1095.
Vincent, J. P., Scharf, S. R. and Gerhart, J. C. (1987). Subcortical rotation in Xenopus eggs: a preliminary study of its mechanochemical basis. *Cell Motil. Cytoskeleton* **8**, 143-154.
Weaver, C. and Kimelman, D. (2004). Move it or lose it: axis specification in Xenopus. *Development* **131**, 3491-3499.
Weaver, C., Farr, G. H., 3rd, Pan, W., Rowning, B. A., Wang, J., Mao, J., Wu, D., Li, L., Larabell, C. A. and Kimelman, D. (2003). GBP binds kinesin light chain and translocates during cortical rotation in Xenopus eggs. *Development* **130**, 5425-5436.
Yarrow, J. C., Lechler, T., Li, R. and Mitchison, T. J. (2003). Rapid de-localization of actin leading edge components with BDM treatment. *BMC Cell Biol.* **4**, 5.
Yisraeli, J. K., Sokol, S. and Melton, D. A. (1990). A two-step model for the localization of maternal mRNA in Xenopus oocytes: involvement of microtubules and microfilaments in the translocation and anchoring of Vg1 mRNA. *Development* **108**, 289-298.
Yost, C., Farr, G. H., 3rd, Pierce, S. B., Ferkey, D. M., Chen, M. M. and Kimelman, D. (1998). GBP, an inhibitor of GSK-3, is implicated in Xenopus development and oncogenesis. *Cell* **93**, 1031-1041.
Yost, H. J. (1991). Development of the left-right axis in amphibians. *Ciba Found. Symp.* **162**, 165-176; discussion 176-181.
Zhou, F. Q., Waterman-Storer, C. M. and Cohan, C. S. (2002). Focal loss of actin bundles causes microtubule redistribution and growth cone turning. *J. Cell Biol.* **157**, 839-849.